# A STUDY OF THE VISCOUS OPTIMIZATION OF THE SHAPE OF A NON-LIFTING STRUT

R.W. DERKSEN & J.G. VEENENDAAL
Department of Mechanical Engineering, University of Manitoba, Canada.

## ABSTRACT

The objective of this work is to gain insight into the process and development of a method for obtaining optimum design shapes for non-lifting aerodynamic struts while employing an interactive viscous-potential flow model for a range of airfoil Reynolds numbers. This was done for axially loaded struts with constant cross-sectional area as well as struts loaded in bending with a fixed cross-sectional moment of inertia. The optimization sought the airfoil shape that resulted in minimum drag. The flow field was obtained by using a panel method that was iteratively coupled to a boundary layer solver. The viscous solver used was to model the boundary layer and was based on the zero-equation, Cebeci-Smith turbulence model. The main flow field was computed using a panel method. The airfoil shape was described using a Bezier-PARSEC shape parameterization and optimization of the shape parameters was obtained using differential evolution. The numerical approach of the flow field solver and the simplicity of the genetic algorithm allowed for these results to be obtained in an acceptable timely manner. This paper will present the results of a number of cases and discuss all of the issues that arose. While one can have confidence in the results, limitations and the need for future work were also exposed. The limitations occurred in this thesis were due to the limitations of the boundary layer flow field solver. This solver did not allow airfoils with significant thickness to be evaluated thus restricting the solution space to thin airfoils. It was observed that future work on dealing with separation modelling needs to be done to allow improved certainty of the optimization.

*Keywords: Aerodynamic optimization, Differential Evolution, Viscous Flow, Bezier-PARSEC*

## 1 INTRODUCTION AND MOTIVATION

Engineers have long sought the ability to obtain designs that obtained peak performance either in minimizing the amount of material used, energy consumed, or other measure of performance. This becomes a question of what is the optimum shape of an aerodynamic configuration to meet a particular objective, such a minimum drag, fixed centre of pressure, and so on. This applies to aircraft, automobiles, building, and any other flow based application one can imagine. Typically, this becomes a question of what is the best shape of a device such as a wing. The relatively recent advent of inexpensive, high performance computers and computation methods has made this possible, but much work needs to be done to develop aerodynamic optimization as a well understood, reliable tool.

The object of this work was to obtain an aerodynamic optimization tool to determine the shapes of a non-lift generating strut for various Reynolds numbers. These struts are used as structural members in a wide variety of applications such as positioning a fan-motor combination in at duct. An additional objective was to gain insight into the interaction of a viscous flow model with the genetic optimization method, Differential Evolution. Here the authors were concerned about the convergence process and quality of the optimized profiles.

Work by Derksen and Bender [1] on determining the shape of axial flow fan nose cones was based on gradient optimization methods. However, it was found that the optimization would quickly be terminated at a local minimum so the optimum shape often depended on the initial configuration. This is not a problem if one is merely looking for a better design, but the optimum solution could not be guaranteed. Hence it was observed that an optimization method that sought out the global optimum was needed.

The current work builds on the previous work of Rogalsky, Derksen, and Kocabiyik [2] and [3] on the inviscid optimization of flow over fan blades. That work sought the shape of the blade that best matched a presumed optimum pressure distribution over the blade. The optimization algorithm used for this work was Differential Evolution, DE, which was found to work very well on these types of problems. A serious deficiency of the earlier work was that the effects of fluid viscosity was neglected even though the use of target pressure distributions had a long history as described by Liebeck and his co-workers [4, 5], and [6]. Rogalsky [7, 8] showed that the use of a Bezier-PARSEC airfoil shape parameterization resulted in faster convergence of the Differential Evolution algorithm for aerodynamic optimization. Differential Evolution is thoroughly described in [9] and [10].

All of the work described above is based on ideal fluid, inviscid and incompressible modelling of the underlying flow. This is believed to be insufficient as real fluids are viscous, which clearly has an effect on the resultant flow solutions. However, it should be made very clear that current, full Navier-Stokes flow simulations require very substantial demands on computational requirements and often result in substantial run times. Additionally, these methods require re-gridding of the flow field which can add a substantial burden to the simulations. The substantial numbers of flow simulations required by any optimization algorithm indicate that these flow simulation schemes unsuitable for optimization for some time. It should be observed that this will change as computer capability improves in the future. The objective of this work was to examine methods that are based on simpler methods. It has been well established that interactive viscous boundary layer – potential schemes have been successful in modelling the flow over airfoils, as discussed by Cebeci [11].

The issue of what the optimization target is for aerodynamic optimization is not as simple as first appears. One can simply look for shapes that minimize drag, the first and most obvious objective. However, this is not always the target. One may seek a shape that produces the greatest lift carrying capability given a fixed thrust. Another choice may be to look for an airfoil that maintains as little change in its centre of pressure over a range of angles of attack or speeds. Wing design is often based on obtaining a configuration that comes as close to an elliptic lift distribution which is shown as an optimum in aerodynamics textbooks. However, Nickel and Wohlfahrt [12] have shown that optimum lift distribution for flying wings was bell shaped. Hence, one must be careful discussing aerodynamic optimization as the results depend on objective.

Based on the previous discussion, it was decided to develop a scheme to optimize the shape of a non-lifting strut. This is a very useful engineering device and clearly has only one optimization objective – minimum drag. The shape of the profile would be based on Bezier-PARSEC parameterization and Differential Evolution would be used as the optimization algorithm. The flow field would be modelled using an interactive Cebeci – Smith boundary layer model coupled to a panel method. The solutions have two constraint scenarios. The first is a constraint on a fixed cross-sectional area which would be a typical requirement for short struts in compression and for struts in tension. This problem requires the cross-sectional area of the strut to be fixed. The other is for fixed cross-section moment of inertia which would be requirement for long struts in compression. Here the section moment of inertia was constrained to a fixed value.

The specific issues that will be discussed are: computational convergence behaviour and iteration time, the characteristics of the shapes generated as a function of Reynolds number, and any concerns or issues regarding the generated cross-sections.

Full details of the work presented here are given by Veenendaal [13].

## 2  COMPUTATIONAL METHOD

A numerical aerodynamic optimization procedure is very easy to describe. It involves relatively few components. The difficulty comes in developing the individual components. The overall process requires the following steps as are shown in Fig. 1.

The first step sets the problem specific parameters such as the cross-sectional area, Reynolds number and so on. The first main code section produces an initial, parent population of candidates. This is done by randomly selecting parameters of a Bezier-PARSEC approximation to the airfoil shape. The Bezier-PARSEC method was selected based on the author's experience. These profiles have to be validated to satisfying their cross-sectional area or moment of inertia. Invalid profiles have their thicknesses amplified by a factor of the square root of the ratio of the required area and the actual area for constant cross-sectional area while the cube root is used for maintaining a target moment of inertia as shown in equations (1) and (2).

Constant area: $$\text{Amplification} = \sqrt{\frac{\text{target area}}{\text{profile area}}}, \text{ and} \qquad (1)$$

Constant Moment: $$\text{Amplification} = \sqrt[3]{\frac{\text{target area}}{\text{profile area}}}. \qquad (2)$$
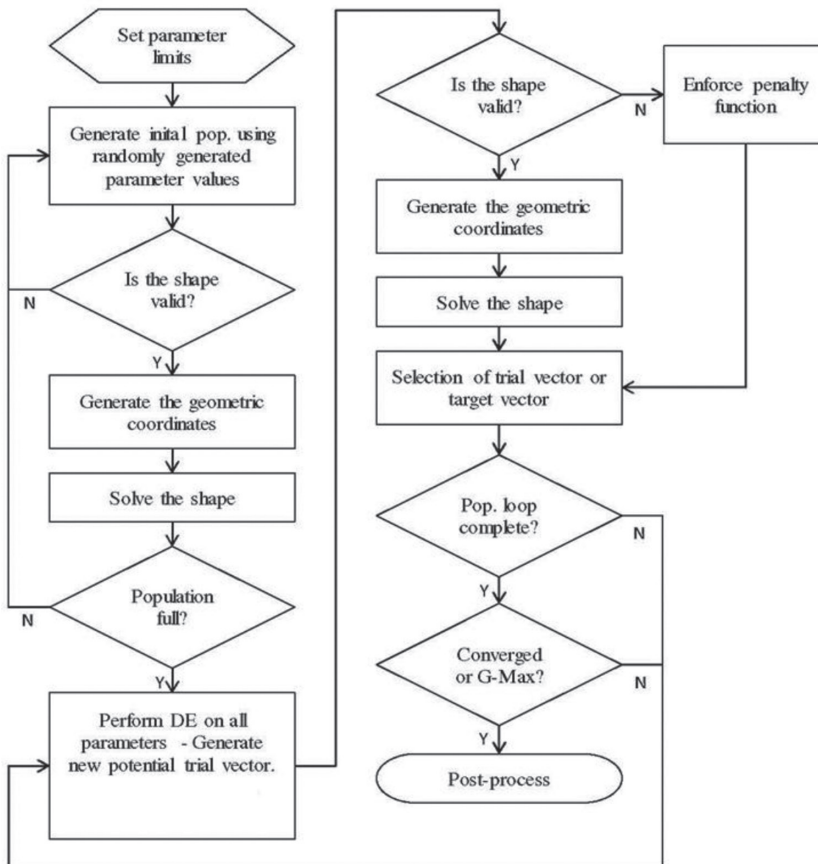


Figure 1: Code Flow Chart.

Part of this process is used to perform a flow field evaluation to determine each member's drag. This is also known as the cost function. This analysis was done using an interactive boundary layer – potential flow method. When the initial population has been generated, the population is then submitted to the Differential Evolution algorithm, which performs a mutation, cross-over, cost function evaluation and tournament process to produce a new child population. This process is continued until the process converges or hits a maximum number of generations. The details of each of the components are discussed in greater detail in the following sections.

## 2.1 Bezier-PARSEC

The thickness distribution employed a BP 3333 as described in [7] and [8]. It has been shown to be a robust and accurate method for determining the shape of an airfoil, as discussed in great detail by Rogalsky [7]. A BP 3333 parameterization uses two third degree Bezier curves to define the thickness distribution. A third degree Bezier curve is given parametrically by eqns (3) and (4).

$$x(u) = x_0(1-u)^3 + 3x_1u(1-u)^2 + 3x_2u^2(1-u) + x_3u^3, \qquad (3)$$

and
$$y(u) = y_0(1-u)^3 + 3y_1u(1-u)^2 + 3y_2u^2(1-u) + y_3u^3, \qquad (4)$$

where $u$ is the parameter that runs from 0 at the beginning to 1 at its terminus. The control points for fourth degree Bezier curves are shown in Fig. 2.

The BP 333 parameterization relies exclusively on the aerodynamic parameters – there are no free Bezier points in BP 3333. The $x_i$ and $y_i$ are the Bezier control points, which are computed from the following:

### 2.1.1 Leading edge thickness curve
The control points are given by

$$x_0 = 0 \qquad\qquad y_o = 0$$

$$x_1 = 0 \qquad\qquad y_1 = 3\kappa_t(x_t - b_9)^2/2 + y_t$$

$$x_2 = b_9 \qquad\qquad y_2 = y_t$$
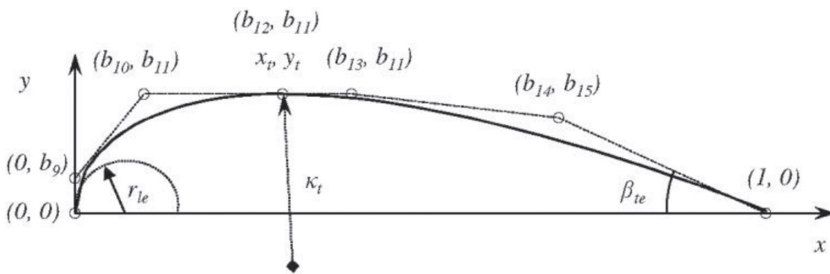
$$x_3 = x_t \qquad\qquad y_3 = y_t$$



Figure 2: Bezier-PARSEC

The parameter $b_9$ is the root of

$$27\kappa_t^2 b_9^4 / 4 - 27\kappa_t^2 x_t b_9^3 + \left(9\kappa_t y_t + 81\kappa_t^2 x_t^2 / 2\right) b_9^2$$
$$+ \left(2r_{le} - 18\kappa_t x_t y_t - 27\kappa_t^2 x_t^3\right) b_9 + \left(3y_t^2 + 9\kappa_t x_t^2 y_t + 27\kappa_t^2 x_t^4 / 4\right) = 0$$

within the bounds given by

$$\max\left(0, x_t - \sqrt{-2y_t / 3\kappa_t}\right) < b_9 < x_t.$$

### 2.1.2 Trailing edge thickness curve
The control points are given by

$$x_0 = x_t \qquad\qquad\qquad\qquad\qquad y_0 = y_t$$
$$x_1 = 2x_t - b_9 \qquad\qquad\qquad\qquad y_1 = y_t$$
$$x_2 = 1 + \left[dz_{te} - \left(3\kappa_t\left(x_t - b_9\right)^2 / 2 + y_t\right)\right]\cot\left(\beta_{te}\right) \qquad y_2 = 3\kappa_t\left(x_t - b_9\right)^2 / 2 + y_t$$
$$x_3 = 1 \qquad\qquad\qquad\qquad\qquad y_3 = dz_{te}$$

The aerodynamics parameters that are embedded in these relations are: $\left(x_t, y_t\right)$ – the location of the thickness crest, $\kappa_t$ – curvature of the thickness crest, $\beta_{te}$ -trailing edge wedge angle, and $dz_{te}$ – the trailing edge thickness, which was forced to $dz_{te} = 0$.

## 2.2 The Interactive Potential – Boundary Layer Flow Solver

The flow field of each population member has to have its drag or cost function evaluated. The method used is that due to Cebeci [11] through the application of his IBL code. This method has been shown to perform well for airfoils that are not subject to separation. It was observed that some of the population members did encounter significant separation. The way this was dealt with was to add a penalty to the computed drag equal to the pressure at the point of separation times the dimensionless thickness at that point. This is very small if the separation is very close to the trailing edge and much more substantial if separation occurs near the maximum thickness. The correction is given in eqn (5)

$$c_d' = c_c + C_p \Delta y. \tag{5}$$

## 2.3 Differential Evolution

In this work a genetic algorithm, Differential Evolution, was used to find the global optimum. The characteristic of this method is that no initial shape needs to be specified as a population of candidate solutions is distributed throughout the solution space. The flow characteristics are then determined using the flow simulation code. The next step in the optimization is to generate a child population which is compared to the parent population. The best is then retained as a next generation and the process is continued till convergence. The constraints are applied when constructing a population member.

Differential Evolution uses the flow chart given in Fig. 3. The DNA of a population member is taken to be an ordered list of the Bezier-Parsec parameters used to describe the shape
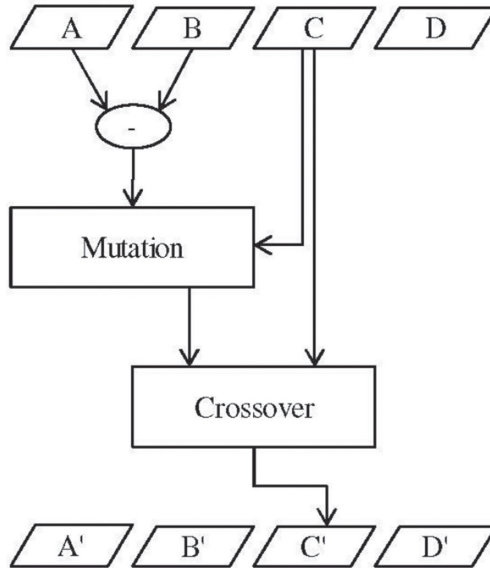
Figure 3: The Differential Evolution Flow Chart.

of the airfoil. Here two randomly selected population members are used to determine a DNA mutation that is the vector difference of the respective DNA. This then multiplied by a factor and added to another population member. The DNA is then subjected to a crossover operation which selectively replaces parameters of the DNA from another population member. The profile would be checked to insure that the area or moment was maintained as a constant.

The candidate child member then had its drag compared to its parent. If the child was fitter it was selected to move on to the next generation, if it was not the parent would be retained. When this was done for each member in the parent population one would have a new generation that would act as a parent population for the next DE round.

The iterations could be terminated in one of three ways. The first is to simply produce a fixed number of generations, and then select the optimum solution from the last generation. This requires a very large number of iterations if one wants to insure convergence. Another method is to compare the optimum solutions from a parent and child population and terminate the iterations when the change is smaller than a specified value. The method that was used in this work is based on the observation that as the iterations proceed the members of a generation cluster about a single point. This is shown in Fig. 4 for a two parameter optimization. Here it was observed that the initial generation is uniformly distributed throughout the solution space. This is desirable as to sample the whole space. The fifth generation is restricted to a smaller portion of the solution space but is still quite dispersed. The 25th generation has the members starting to appear to converge on three locations. It is quite clear from the converged solution all of the population members converged to a single point. Thus one has convergence when the mean square of the distances between a population member and all of the others is less than a specified value. One should note that if this distance does not continue to decrease one may have multiple locations for the minimum. This was not observed for the problem of determining the shape with minimum drag.
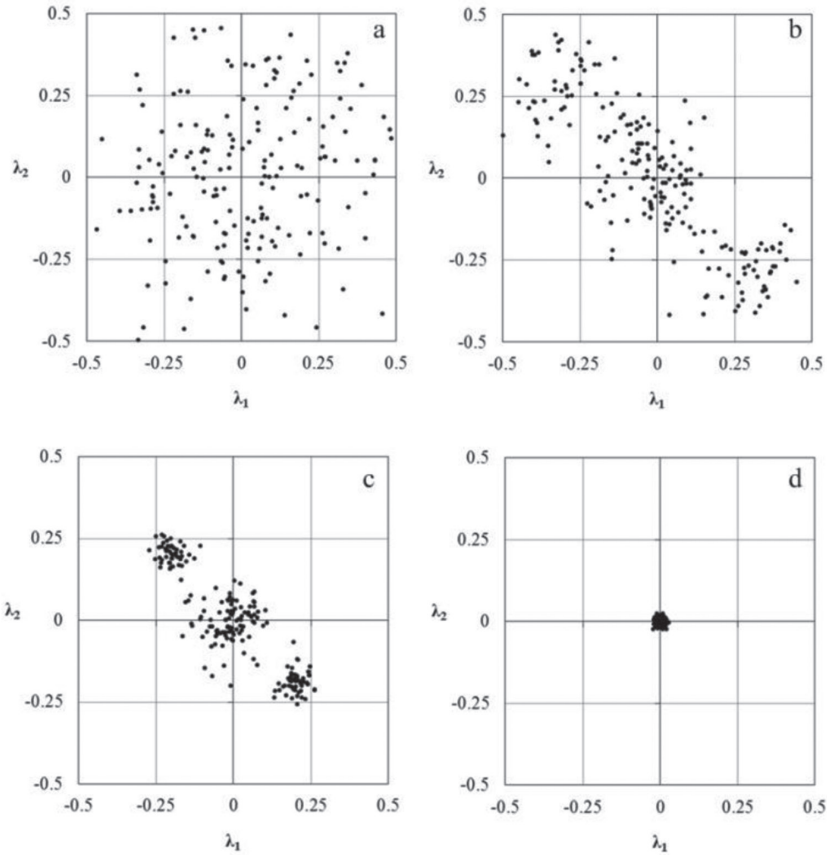
Figure 4: Location of a DE generation's members: a) the initial population, b) fifth generation, c) 25th generation, and d) converged generation.

The specific DE parameters used in this work were a population size of 100, a mutation scaling factor of $F = 0.3$, and a crossover constant of $CR = 0.8$. A limit of a maximum of 500 generations was also used.

## 3 RESULTS

A large number of different cases were examined in [13] and cannot all be presented here. Hence a representative subset is given and discussed. These cases demonstrated the characteristics that were found in the larger body of work that was done. The optimum strut shapes with a fixed area and different Reynolds numbers are given in Figs 5 and 6. While the optimum strut shapes with a fixed moment and different Reynolds numbers are given in Figs 7 and 8.

The optimum strut profiles were typically found after approximately 80 to 150 generations. This represents 8,000 to 15,000 flow field simulations which clearly demonstrates the unsuitability of elaborate flow solution methods. This is encouraging to other viscous flow optimization processes as the number of flow field simulation is not too large for simple flow field simulation methods.
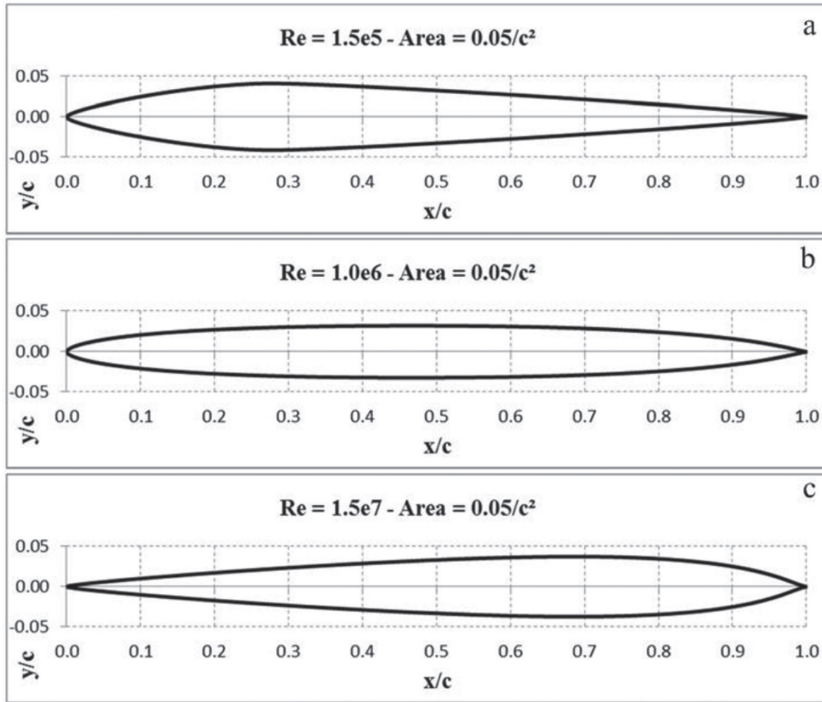
Figure 5: Fixed area case $a = 0.05 / c^2$. a) Re $= 150,000$. b) Re $= 1,000,000$. c) Re $= 15,000,000$.

Figure 5 is the fixed area case where the non-dimensional area is 5% of the square of the chord length. The change of the profiles with Reynolds number is quite interesting. One can observe that the maximum thickness for the lowest Reynolds number, Fig. 5a, is at roughly 30% of the chord length which is characteristic of NACA four digit airfoils. Here the forward portion of the strut is curved, while the trail portion appears to be quite linear. The result for the intermediate Reynolds number, Fig. 5b, has its maximum thickness at roughly 50% chord, with both the leading and trailing portions of the profile being curved. Interestingly, the shape of the strut for the largest Reynolds number, Fig. 5c, has its maximum thickness at roughly 70% chord and looks very much like a backward airfoil. One can hypothesize that the rearward motion of the maximum thickness exploits having a larger extent of laminar boundary layer. The shape at the maximum Reynolds number is more difficult to explain. While it may be a legitimate shape, in may suffer from the flow solver's inability to properly address separation, and the penalty assessed being inadequate. This is an issue that needs to be addressed by either improving the separation modelling of the iterative current solver, or using a higher order flow simulation method.

Figure 6 demonstrates that similar behaviour for a strut that has a cross-sectional area 10% of the chord length squared is observed. This is consistent with the results shown in Fig. 5. The low Reynolds number profile is typical of a traditional airfoil with a maximum thickness at roughly 40% of the chord length. The high Reynolds number profile has a maximum thickness at roughly 65% of the chord length, while the profile appears to be quite pinched following the maximum thickness. Again, this could be the result of deficiencies in the flow solver and drag penalty.
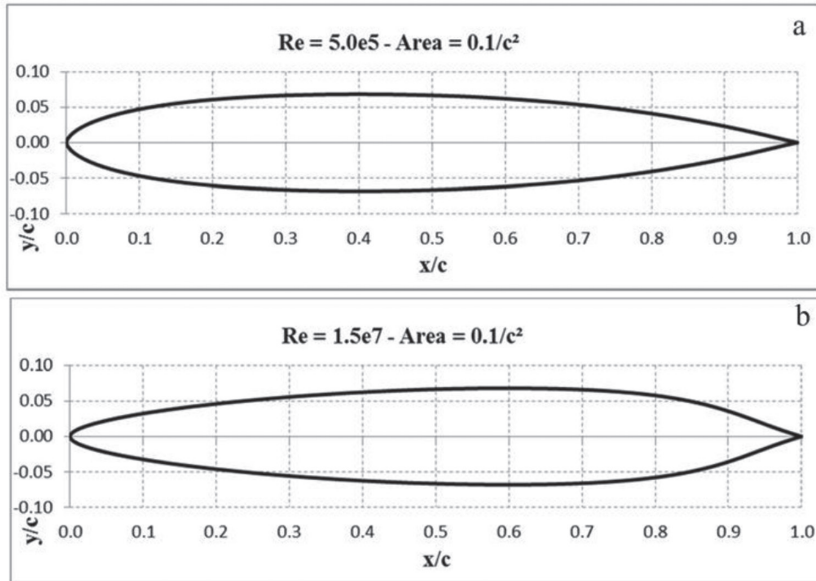
Figure 6: Fixed area case $a = 0.1/c^2$. a) Re $= 500,000$. b) Re $= 15,000,000$.

The first of the fixed moment cases is shown in Fig. 7. As for the fixed area problem, it was observe that the maximum thickness of the profile moves back along the chord line. The profiles have a near diamond shape in Figs 7a and 7b. A more traditional profile is observed in Fig. 7c, while a reversed airfoils shape is found in Fig. 7d. Again this supports the observation that for the lower Reynolds number, the strut profiles are exploiting a larger length of laminar boundary layer to minimize drag. This may still be true of the largest Reynolds number, but flow simulation issues may also be at play.

The final example of maintaining a fixed cross-sectional moment is shown in Fig. 8. Here the maximum thickness is at 20% of chord length if the Reynolds number is 200,000 and at roughly 50% for a Reynolds number of 1,500,000. This figure mirrors the trends shown previously; however, one does not observe a reversed airfoil as the Reynolds numbers are large enough.

A more detailed study of the Bezier-PARSEC parameters was performed for constant area and constant moment. The behaviour are qualitatively similar, so only the results for constant area will be presented.

The location of the optimum strut is shown in Fig. 9. The areas varied from 0.05 to 0.15 times the chord length squared, and the Reynolds numbers varied from $4 \times 10^4$ to roughly $1 \times 10^7$. The range of Reynolds numbers is restricted for the larger struts due to separation issues. For the smallest cross-section it was observed that the location of maximum thickness is nearly constant at low Reynolds number. However, the trend clearly indicates that this positon is pushed toward the trailing edge for higher Reynolds numbers and for all of the remaining cases.

The variation of the maximum thickness shown in Fig. 10 indicates that the maximum thickness, while a function of cross-sectional area, is only weakly influenced by Reynolds number.

The trailing edge wedge angle is shown in Fig. 11. Here it was observed that this angle increases with Reynolds number for all cases. It should be noted that the maximum wedge
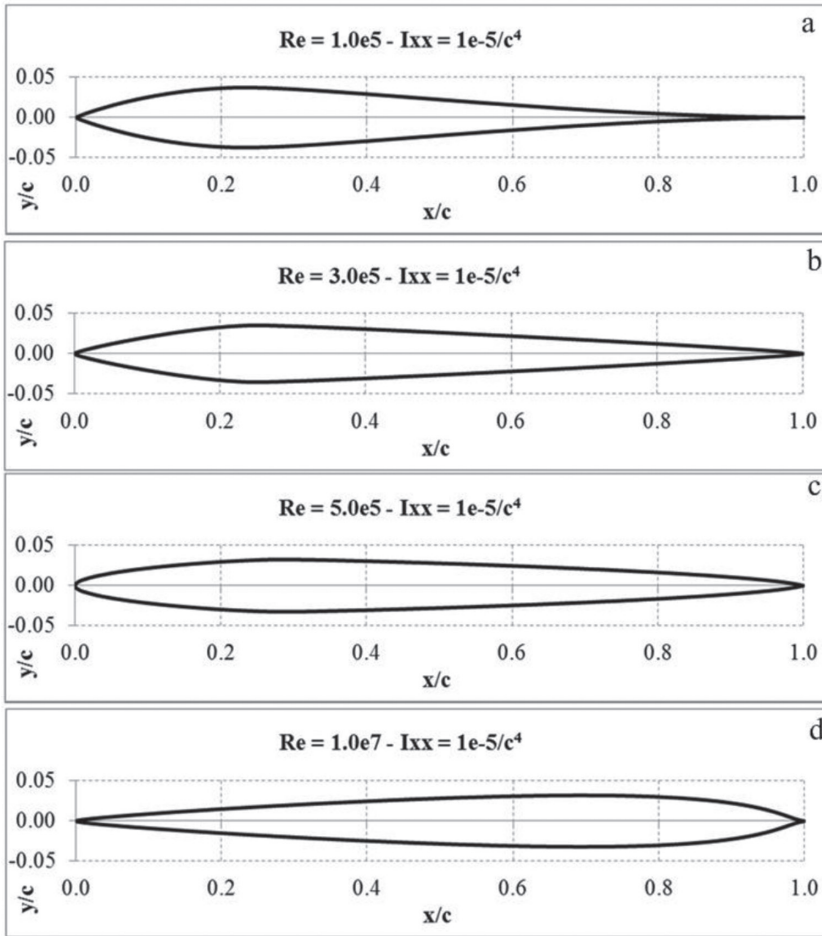
Figure 7: Fixed moment case $I_{xx} = 1.0 \times 10^{-5} / c^4$. a) Re $= 100,000$. b) Re $= 300,000$. c) Re $= 500,000$. d) Re $= 10,000,000$.
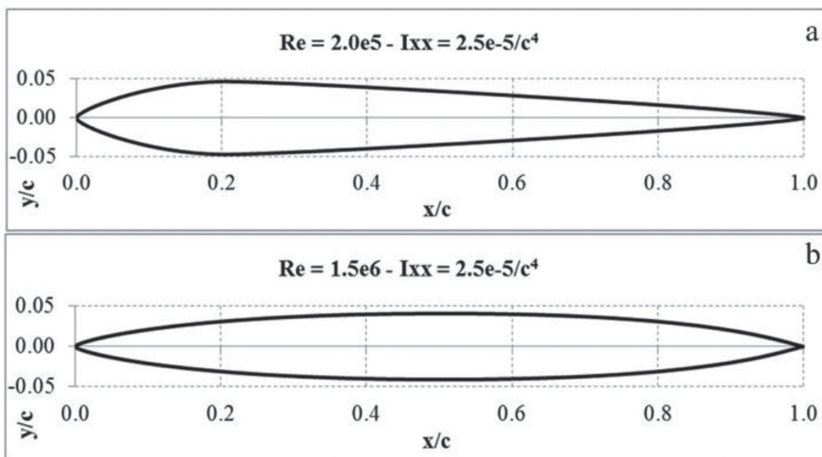


Figure 8: Fixed moment case $I_{xx} = 2.5 \times 10^{-5} / c^4$. a) Re $= 200,000$. b) Re $= 1,500,000$.
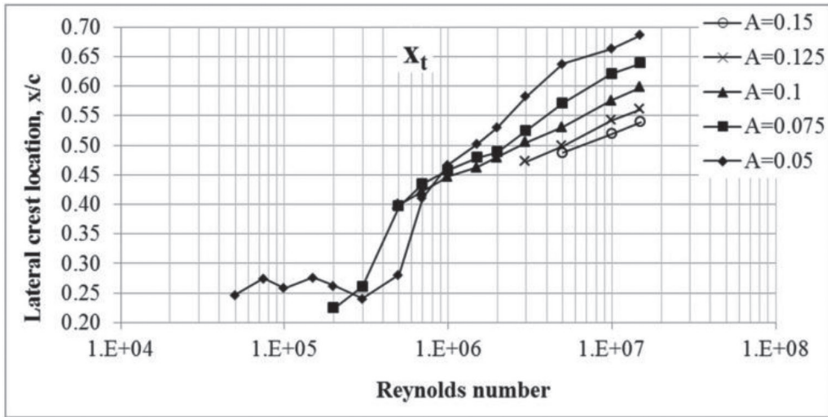
Figure 9: The shift in location of the maximum thickness location with Reynolds number for various fixed cross-sectional area.
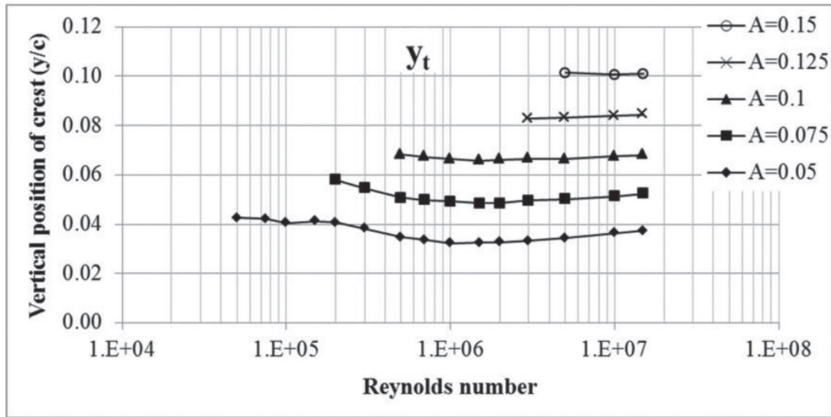


Figure 10: The variation of the maximum thickness with Reynolds number for various fixed cross-sectional area.
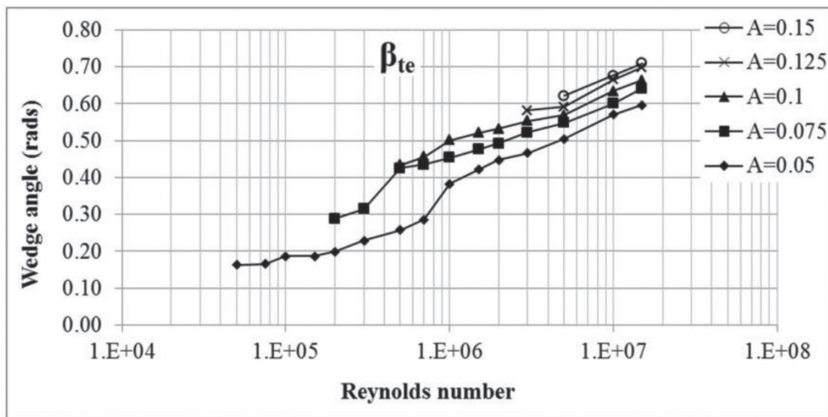


Figure 11: The of the trailing edge wedge angle with Reynolds number for various fixed cross-sectional area.

angle obtained was $40°$ which is larger than one would expect for an airfoil. This may be a result of the issues related to flow separation and the penalty method used to deal with it. This does indicate that the flow field analysis has to be improved to deal with separation at the larger Reynolds number. It should be noted that the optimization process will select a flawed solution if the drag computed is small.

The next step in determining the optimum shape of a strut, or any airfoil, requires work on adding a module to model the separated region of the flow field.

## 4 CONCLUSIONS

One can conclude that this method is a profitable one for determining optimum aerodynamic struts and potentially airfoils. Execution times are reasonable, and for lower Reynolds numbers reasonable strut profiles are generated. While one cannot automatically discount the higher Reynolds number struts, one can suspect that improvements to the flow field modelling are required to deal with separation. The general observation regarding a strut is that the maximum thickness is nearly constant and moves toward the trailing edge as the required Reynolds number increases.

## REFERENCES

[1] Derksen, R.W. & Bender, J.R., Aerodynamic shape optimisation of axial flow fan nose cones. *Computer Aided Optimization in Engineering XII*, WIT Transactions on the Built Environment, Vol. 125, New Forest, UK, pp. 109–118, 2012.

[2] Rogalsky, T., Derksen, R.W. & Kocabiyik, S., An aerodynamic design technique for optimizing fan blade spacing. *Proceedings of the 7th Annual Conference of the Computational Fluid Dynamics Society of Canada*, pp. 2.29–2.34, 1999.

[3] Rogalsky, T., Derksen, R.W. & Kocabiyik, S., Differential evolution in aerodynamic optimization. *Canadian Aeronautics and Space Journal*, **46**(4), pp. 183–190, 2000.

[4] Liebeck, R.H. & Ormsbee, A.I., Optimization of airfoils for maximum lift. *Journal of Aircraft*, **7**(5), pp. 409–415, 1970.
https://doi.org/10.2514/3.44192

[5] Liebeck, R.H., A class of airfoils designed for high lift in incompressible flow. *Journal of Aircraft*, **10**(10), pp. 610–617, 1973.
https://doi.org/10.2514/3.60268

[6] Liebeck, R.H., Design of subsonic airfoils for high lift. *Journal of Aircraft*, **15**(9), pp. 547–561, 1978.
https://doi.org/10.2514/3.58406

[7] Rogalsky, T., *Acceleration of Differential Evolution for Aerodynamic Design*, Ph.D., University of Manitoba, 2004.

[8] Derksen, R.W. & Rogalsky, T., Optimum airfoil parameterization for aerodynamic design, *Computer Aided Optimum Design in Engineering XI*, WITPress, New Forest, UK, pp. 197–206, 2009.

[9] Corne, D., Dorigo, M. & Glover, F. (eds), *New Ideas in Optimization*, McGraw-Hill, London, pp. 77–158, 1999.

[10] Feoktistov, V., *Differential Evolution in Search of Solutions*, Springer-Verlag, New York, 2006.

[11] Cebeci, T., *Turbulence Models and Their Applications*, Springer-Verlag, Berlin, 2003.

[12] Nickel, K. & Wohlfahrt, M., *Tailless Aircraft in Theory and Practice*, AIAA, Washington, 1994.

[13] Veenendaal, J.G., *Aerodynamic Design Optimization of a Non-Lifting Strut*, M.Sc. Thesis, University of Manitoba, 2014.